Inorganic Chemistry

Article

pubs.acs.org/IC

Theoretical Investigation into the Mechanism of 3′-dGMP Oxidation by [$Pt^{IV}Cl_4$(dach)]

Alireza Ariafard,*[,†] Narges Mahdizadeh Ghohe,[†] Kiana Khadem Abbasi,[†] Allan J. Canty,[‡] and Brian F. Yates*[,‡]

[†]Department of Chemistry, Faculty of Science, Central Tehran Branch, Islamic Azad University, Shahrak Gharb, Tehran, Iran

[‡]School of Chemistry, University of Tasmania, Private Bag 75, Hobart TAS 7001, Australia

Supporting Information

ABSTRACT: The mechanism for the oxidation of 3′-dGMP by [$PtCl_4$(dach)] (dach = diaminocyclohexane) in the presence of [$PtCl_2$(dach)] has been investigated using density functional theory. We find that the initial complexation, i.e., the formation of [$PtCl_3$(dach)(3′-dGMP)], is greatly assisted by the reaction of the encounter pair [$PtCl_2$(dach)···3′-dGMP] with [$PtCl_4$(dach)], leading to migration of an axial chlorine ligand from platinum(IV) to platinum(II). A dinuclear platinum(II)/platinum(IV) intermediate could not be found, but the reaction is predicted to pass through a platinum(III)/platinum(III) transition structure. A cyclization process, i.e., C8−O bond formation, from [$PtCl_3$(dach)(3′-dGMP)] occurs through an intriguing phosphate−water-assisted deprotonation reaction, analogous to the opposite of a proton shuttle mechanism. Followed by this, the guanine moiety is oxidized via dissociation of the Pt^{IV}−Cl_{ax} bond, and the cyclic ether product is finally formed after deprotonation. We have provided rationalizations, including molecular orbital explanations, for the key steps in the process. Our results help to explain the effect of [$PtCl_4$(dach)] on the complexation step and the effect of a strong hydroxide base on the cyclization reaction. The overall reaction cycle is intricate and involves autocatalysis by a platinum(II) species.

INTRODUCTION

DNA oxidative damage,[1] which leads to processes such as aging, mutagenesis, and carcinogenesis,[2] can be induced by many transition-metal complexes.[3] One of the transition-metal complexes that has the potential to oxidize DNA is [$Pt^{IV}Cl_4$(dach)] (**1**). Choi and co-workers proposed this platinum(IV) complex as a highly reactive agent for oxidation of the guanine (G) moiety of DNA.[4] They showed that only G nucleotides having a hydroxyl or a phosphate as a nucleophile in the 5′ position can be oxidized by platinum(IV), for example, 5′-dGMP, 3′-dGMP, and 5′-[GTTTT]-3′ and not cGMP, 9Mxan, 5′-d[TTGTT]-3′, and 5′-d[TTTTG]-3′. However, it should be mentioned that such an oxidation reaction may not necessarily be biologically relevant because the short half-life of **1** in both in vivo and in vitro conditions reduces the likelihood of its interaction with cellular DNA.[5,6]

The experimentally postulated reaction mechanism for the oxidation of 5′-dGMP and 3′-dGMP by **1** was explored by Choi and co-workers.[4c,d] Followed by this, we conducted a theoretical investigation into the oxidation of 5′-dGMP by **1**.[7] From these two independent works, the following reaction mechanism for G oxidation can be proposed (Scheme 1). The first step of this reaction is the binding of N7 of G to Pt^{IV} via the substitution of one of the Cl_{ax} ligands of **1** by 5′-dGMP. The resulting complex (**2_5′G**) then undergoes an intramolecular nucleophilic attack, producing intermediate **3_5′G**. From this intermediate, two electrons are easily transferred from G to Pt^{IV} by lengthening of the Pt−Cl_{ax} bond, releasing the cationic phosphodiester **4_5′G**, thereby oxidizing G. Finally, the cationic phosphodiester intermediate is deprotonated by water and then hydrolyzed to the final product 8-oxo-5′-dGMP.

As mentioned above, in order for the redox reaction to occur, one of the Cl_{ax} ligands of **1** should be initially replaced by G. Generally, substitution reactions for a d^6 octahedral platinum complex proceed through a dissociative mechanism and are usually very energy-consuming. However, Choi and co-workers showed that the substitution reaction can be greatly accelerated by the addition of a platinum(II) complex such as [$Pt^{II}Cl_2$(dach)] (**2**).[4e,f] They confirmed that the substitution reaction is catalyzed by the platinum(II) complex via the Basolo−Pearson (BP) mechanism (Scheme 2).[8] This mechanism has also been reported by other researchers.[5,9] According to this mechanism (Scheme 2), the five-coordinate platinum(II) complex [$Pt^{II}Cl_2$(dach)G] (**3**) is supposed to form first through the coordination of N7 of G to Pt^{II}. Subsequently, one of the Cl_{ax} ligands (and not Cl_{eq}) of **1** is coordinated to the sixth position of **3**, forming the binuclear complex **4**. In the binuclear species, the two-electron transfer from Pt^{II} to Pt^{IV} is associated with the Cl_{ax} transfer from Pt^{IV} to Pt^{II}, giving the ligand substitution product **5** and regenerating the platinum(II) complex **2**.[4e,f] As shown in Scheme 1, the platinum(II) complex **2** is also generated through two-electron transfer from G to

Received: August 22, 2012
Published: December 27, 2012

dx.doi.org/10.1021/ic3018425 | Inorg. Chem. 2013, 52, 707−717

Scheme 1

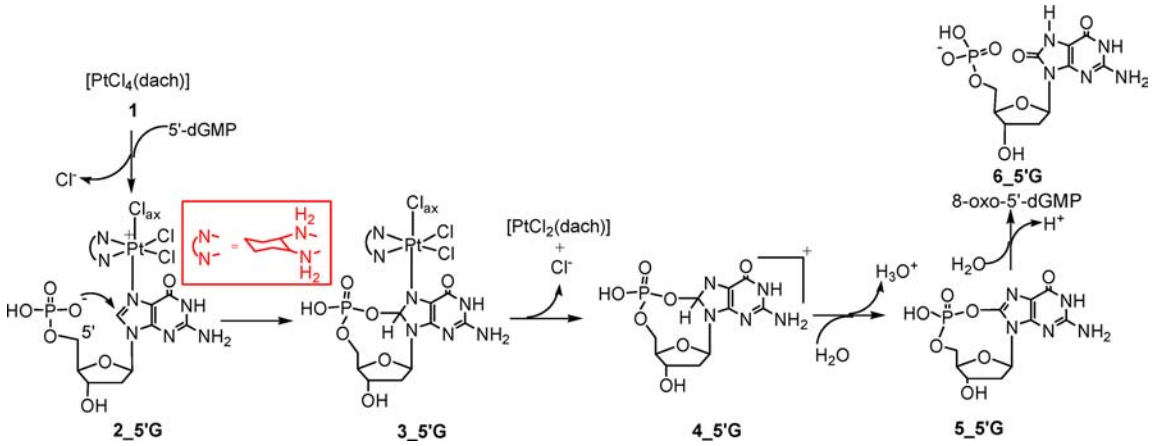

Scheme 2

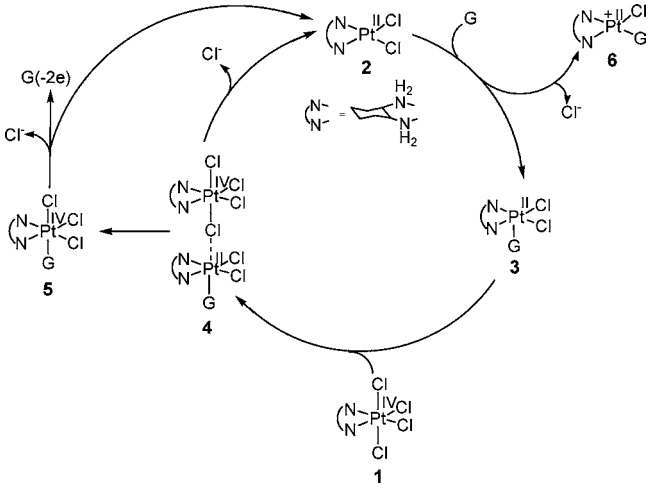

Pt^{IV}. Because one of the final products of the redox reaction, **2**, is the catalyst for the substitution reaction, the overall redox reaction is called autocatalytic. However, it should be mentioned here that the formation of **5** from **2** is subject to competition with the substitution of one of the Cl ligands of **2** by G to form **6**.[4c,d]

For the oxidation of 3′-dGMP, the reaction mechanism depicted in Scheme 3 was proposed by Choi and co-workers.[4d] They suggested that, after replacement of a Cl_{ax} by 3′-dGMP, the nucleophilic attack of the alcohol functional group (−OH) to C8 is followed by two-electron transfer from G to Pt^{IV}, deprotonation of both the C8−H and O−H bonds, and

Scheme 3

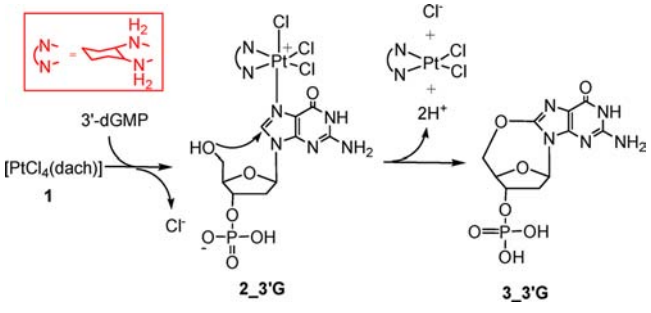

eventually the formation of cyclic ether **3_3′G** as the final product.

In this study, we utilize density functional theory (DFT) to elucidate the reaction mechanism of 3′-dGMP oxidation by **1**. Through this work, we show how substitution, deprotonation, and electron-transfer events occur during the overall redox reaction. Our hope is that the results of this study will assist with understanding the oxidation of other nucleotides and duplex DNA.

COMPUTATIONAL DETAILS

Gaussian 09[10] was used to fully optimize all of the structures reported in this paper in water using the conductor-like polarizable continuum model (CPCM) solvation model[11] at the B3LYP level of DFT.[12] The effective core potential of Hay and Wadt with a double-ξ valence basis set (LANL2DZ)[13] was chosen to describe Pt. The 6-31G(d) basis set was used for other atoms.[14] A polarization function of ξ_f = 0.993 was also added to Pt.[15] This basis set combination will be referred to as BS1. Frequency calculations were carried out at the same level of theory as that for structural optimization. Intrinsic reaction coordinate[16] calculations were used to confirm the connectivity between transition structures and minima. Because recent studies have established that M06[17] predicts the activation energies more accurately than B3LYP,[7,18] we carried out single-point energy calculations for all of the structures with a larger basis set (BS2) at the M06 level. BS2 utilizes the quadruple-ζ valence def2-QZVP[19] basis set on Pt and the 6-311+G(2d,p) basis set on other atoms. The solvation energies were calculated using BS2 on optimized geometries with the CPCM solvation model using water as the solvent. To estimate the corresponding Gibbs free energies, ΔG, the entropy corrections were calculated at the B3LYP/BS1 level, adjusted by the method proposed by Okuno,[20] and finally added to the M06/BS2 total energies. We have used the potential and Gibbs free energies obtained from the M06/BS2//B3LYP/BS1 calculations in water throughout the paper unless otherwise stated. The atomic orbital populations were calculated on the basis of natural bond orbital (NBO) analyses.[21]

RESULTS AND DISCUSSION

Substitution Reaction of Cl_{ax} of 1 by 3′-dGMP. In order for the oxidation of 3′-dGMP by Pt^{IV} to take place, one of the chloride ligands of Pt^{IV} should be initially replaced by 3′-dGMP. As discussed in the Introduction, the replacement is known to be catalyzed by a platinum(II) complex.[4e,f] Figure 1a compares the energy profiles for the substitution reaction through dissociative and Pt^{II}-catalyzed pathways.

Our calculations show that the dissociation pathway involving the loss of one of the Cl ligands from **1** requires

dx.doi.org/10.1021/ic3018425 | Inorg. Chem. 2013, 52, 707−717

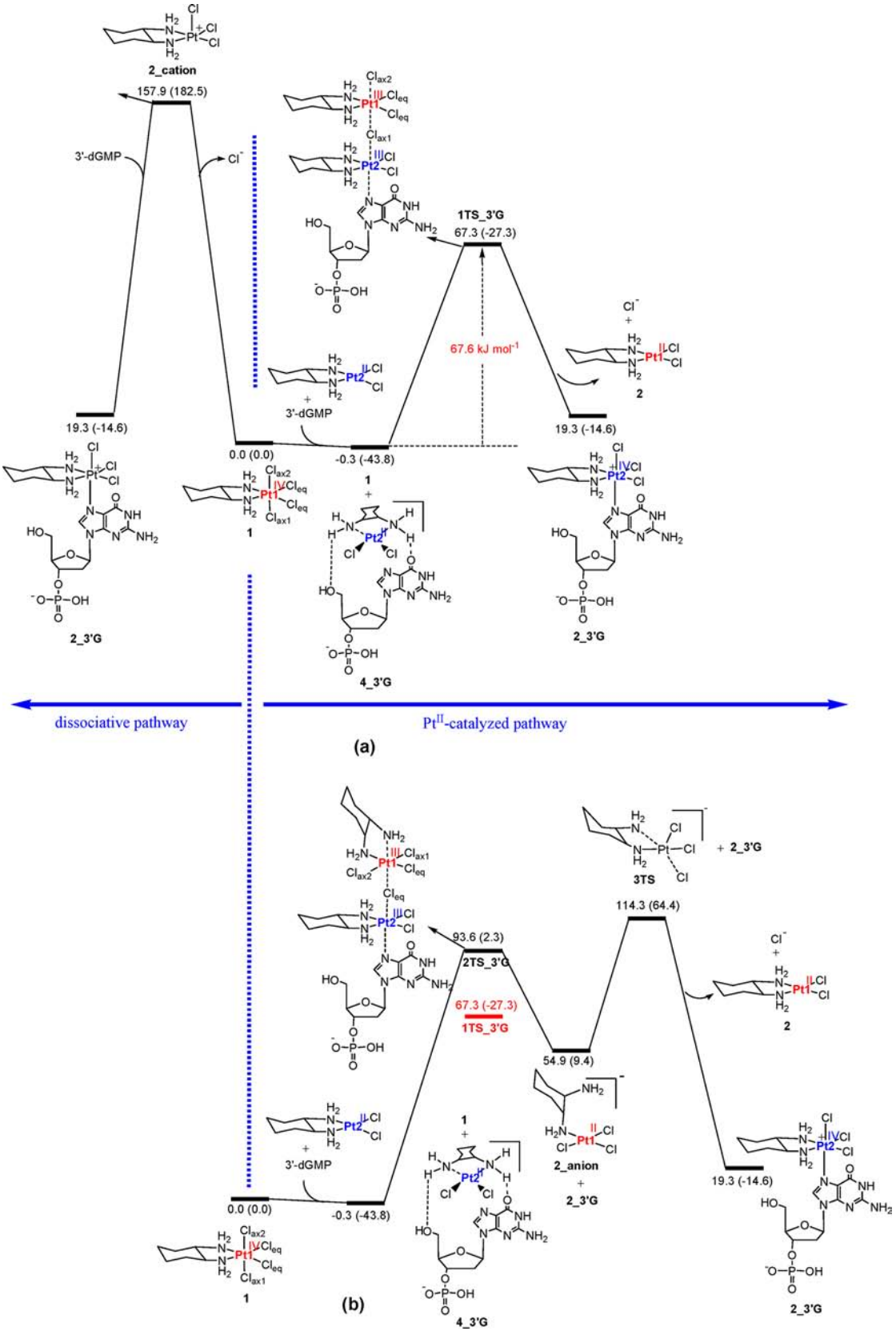

Figure 1. Energy profiles calculated for the substitution of one of the Cl_{ax} ligands of **1** by 3′-dGMP through (a) the dissociative pathway and the Pt^{II}-catalyzed pathway in which a Cl_{ax} ligand is transferred from **1** to **2** and (b) the Pt^{II}-catalyzed pathway in which a Cl_{eq} ligand is transferred from **1** to **2**. The relative free and electronic energies (in parentheses) obtained from the M06/BS2//B3LYP/BS1 calculations in water are given in kJ mol^{-1}.

overcoming an energy barrier as high as 157.9 (182.5) kJ mol^{-1}, suggesting that this pathway is less likely to occur (the relative free energy is reported along with the relative electronic energy in parentheses). In contrast, the substitution reaction via the

dx.doi.org/10.1021/ic3018425 | Inorg. Chem. 2013, 52, 707−717

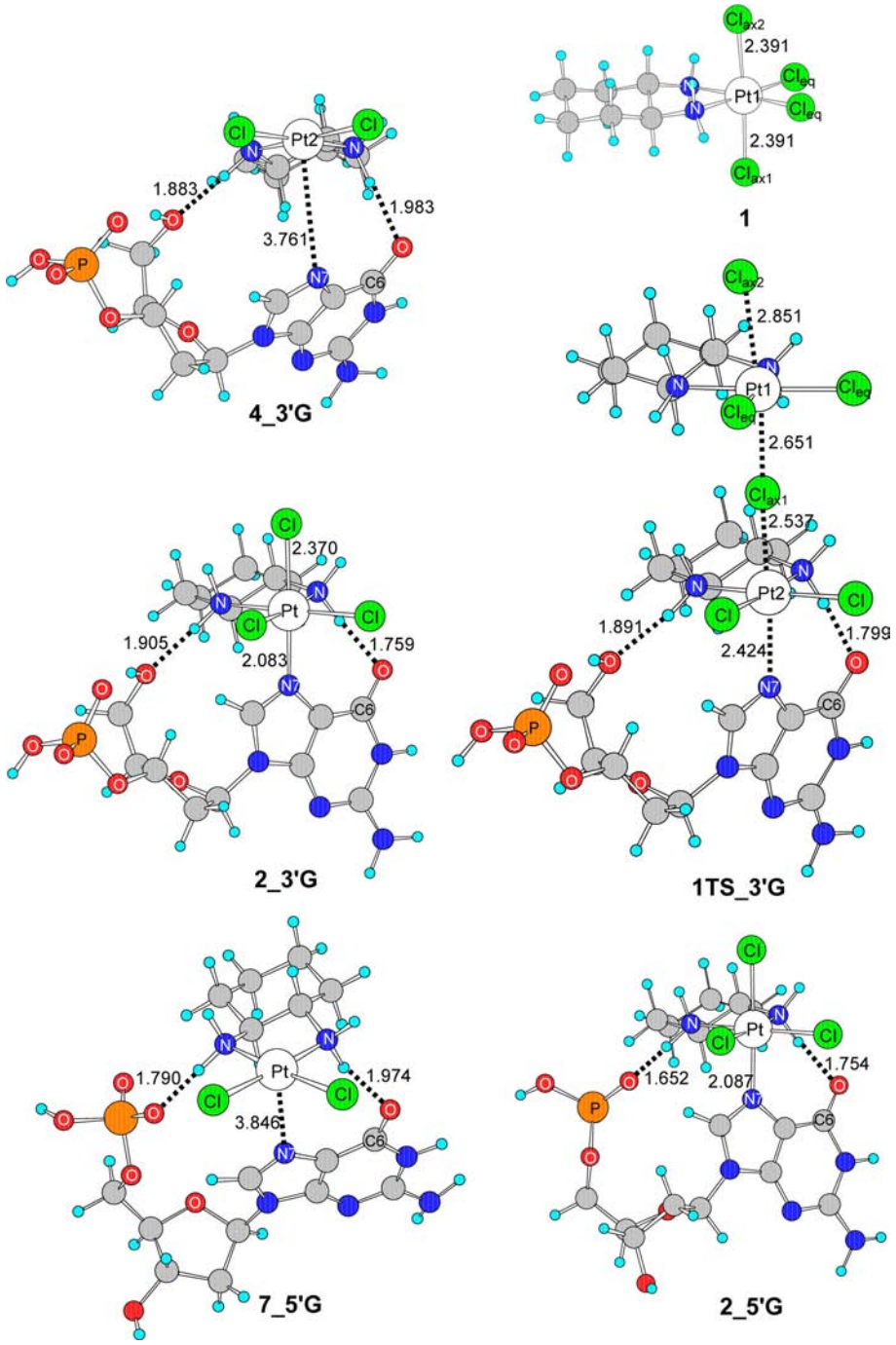

Figure 2. Optimized structures with selected structural parameters (bond lengths in angstroms) for **1**, **4_3′G**, **1TS_3′G**, **2_3′G**, **2_5′G**, and **7_5′G**.

Pt^{II}-catalyzed pathway needs a much lower activation energy (67.3 kJ mol^{-1} at the transition structure **1TS_3′G**), indicating that this pathway is much more favorable than the dissociation pathway (Figure 1a).

In the literature, the first step of the Pt^{II}-catalyzed pathway is assumed to be coordination of the G N7 atom to the Pt^{II} center to form a five-coordinate intermediate.[4e,f] Attempts to locate such an intermediate were unsuccessful; all optimizations starting from a five-coordinate complex converged to the encounter pair **4_3′G**, wherein no bond exists between Pt^{II} and N7; the Pt−N7 distance in **4_3′G** is calculated to be as long as 3.761 Å (Figure 2). Indeed, a five-coordinate complex is found to be a transition state and not an intermediate (vide infra). In the encounter pair **4_3′G**, **2** and 3′-dGMP are attached together via hydrogen bonding; the N−H protons of the dach ligand interact simultaneously with the C6O carbonyl and hydroxyl group (Figure 2).[22] These hydrogen bonds are preserved during the substitution reaction. As the final step of the substitution reaction, the bridged transition structure **1TS_3′G** is formed through interaction of the Cl_{ax1} ligand of **1** with Pt^{II} (Figure 1a). In this transition structure, the Pt2−N7 and Pt2−Cl_{ax1} bonds start to form, while the Pt1−Cl_{ax1} and Pt1−Cl_{ax2} bonds start to break (Figure 2). NBO analysis shows that the Pt2 d_{z^2} orbital is depopulated upon going from **4_3′G** (1.878) to **1TS_3′G** (1.501) and then to **2_3′G** (1.220), while the Pt1 d_{z^2} orbital is populated upon going from **1** (1.273) to

dx.doi.org/10.1021/ic3018425 | *Inorg. Chem.* 2013, 52, 707−717

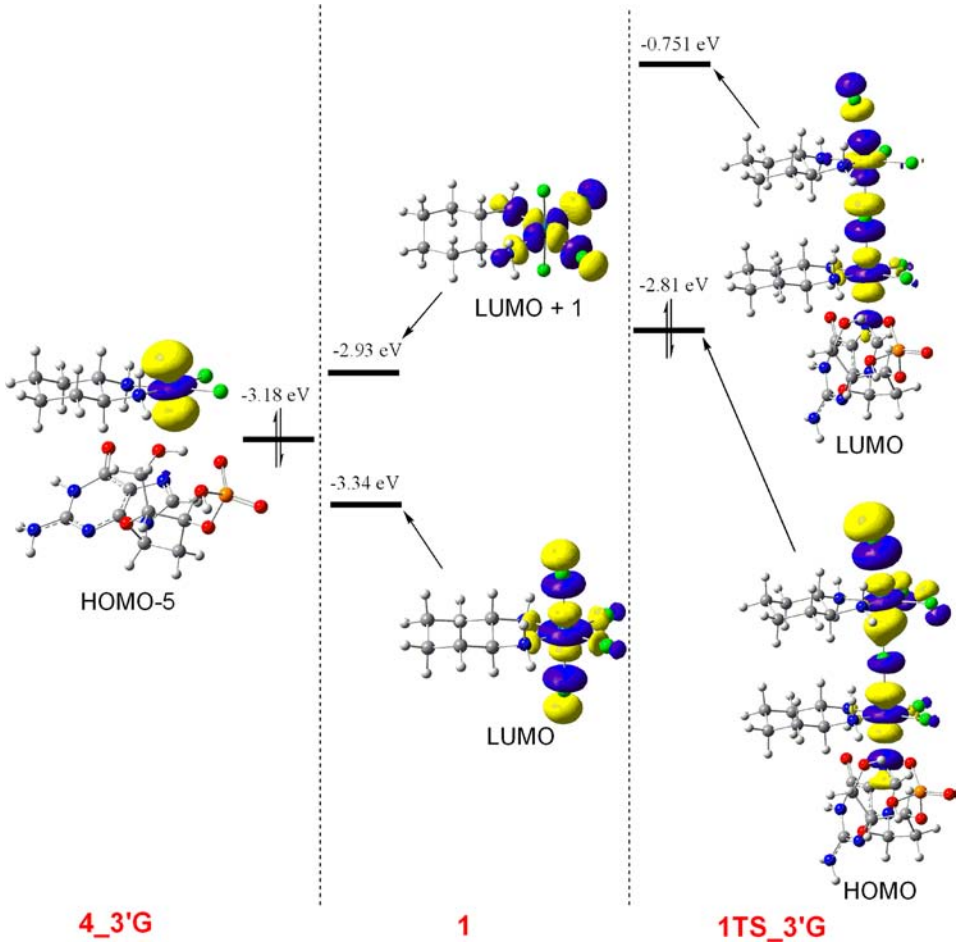

Figure 3. Spatial plots and energies of (a) HOMO−5 of **4_3′G**, (b) LUMO and LUMO+1 of **1**, (c) and HOMO and LUMO of **1TS_3′G**.

1TS_3′G (1.529) and then to **2** (1.875). This supports the fact that electron transfer occurs from the Pt2 d_{z^2} orbital of **4_3′G** to Pt1 d_{z^2} orbital of **1**, mainly through interaction of the sixth highest occupied molecular orbital HOMO-5 of **4_3′G** with the lowest unoccupied molecular orbital (LUMO) of **1** (Figure 3). This type of interaction gives rise to two bonding and two antibonding orbitals.[23] As shown in Figure 3, one of these two antibonding orbitals (HOMO of **1TS_3′G**) is doubly occupied and lies 0.37 eV above HOMO−5 of **4_3′G**. Thus, the binuclear **1TS_3′G** is a transition structure and not a local minimum (intermediate). Because the contributions of the atomic d_{z^2} orbitals of Pt1 and Pt2 to the HOMO of **1TS_3′G** are almost equal, the bonding character of this transition structure can be described as Pt^{III}−Cl−Pt^{III}. However, after crossing the transition structure **1TS_3′G**, the electron-transfer process is completed and **2_3′G** is formed via migration of the Cl_{ax1} ligand from Pt1 to Pt2.

Pt^{II}-Catalyzed Substitution Reaction via the Migration of Cl_{eq} to Pt^{II}. Choi and co-workers showed that during the substitution reaction, only a Cl_{ax} ligand is transferred from Pt^{IV} to Pt^{II} and not a Cl_{eq} ligand.[4f] This suggests that electron transfer through the Cl_{ax}−Pt^{IV}−Cl_{ax} axis is much easier than that through the Cl_{eq}−Pt^{IV}−N axis. Our calculations provide further support to this experimental finding (Figure 1b); **2TS_3′G** is computed to be 26.3 kJ mol^{-1} higher in energy than **1TS_3′G**. We found that if the Pt d_{z^2} orbital of **4_3′G** interacts with the Pt $d_{x^2-y^2}$ orbital of **1**, electron transfer occurs through the Cl_{eq}−Pt^{IV}−N axis. Because, in **1**, the $d_{x^2-y^2}$ orbital (LUMO+1) is about 0.41 eV higher in energy than the d_{z^2} orbital (LUMO; Figure 3), electron transfer to Pt^{IV} through the Cl_{eq}−Pt^{IV}−N axis is energetically more demanding. Indeed, the more significant antibonding interaction between orbitals of N and Pt causes $d_{x^2-y^2}$ to lie above d_{z^2} and be less available.

Pt^{II}-Catalyzed Substitution Reaction of Cl_{ax} by 5′-dGMP. For the sake of completeness, we also extended the calculations to study the Pt^{II}-catalyzed substitution reaction of Cl_{ax} by 5′-dGMP (Figure 4). Our calculations show that the formation of the encounter pair **7_5′G** (Figure 4) is about 18.5 kJ mol^{-1} more favorable than that of the encounter pair **4_3′G** (Figure 1a). The same is true for the substitution reaction products; **2_5′G** (Figure 4) is calculated to lie 46.0 kJ mol^{-1} below **2_3′G** (Figure 1a). These results suggest that the hydrogen bonds between 5′-dGMP and dach are stronger than those between 3′-dGMP and dach. This is because the NH_2 moiety interacts with the phosphate group better than the hydroxyl group, a claim that is supported by shorter H···O(phosphate) distances in **7_5′G** (1.790 Å) and **2_5′G** (1.652 Å) versus the H···O(hydroxyl) distances in **4_3′G** (1.883 Å) and **2_3′G** (1.905 Å) (Figure 2). This difference could be related to the higher basicity of the phosphate group relative to the hydroxyl group.

We also found that the energy required for the transformation of **7_5′G** + **1** to **1TS_5′G** (67.9 kJ mol^{-1}; Figure 4) is very close to that for the transformation of **4_3′G** + **1** to **1TS_3′G** (67.6 kJ mol^{-1}; Figure 1a). This is entirely consistent with the experimental findings of Choi and co-workers; the

dx.doi.org/10.1021/ic3018425 | *Inorg. Chem.* 2013, 52, 707−717

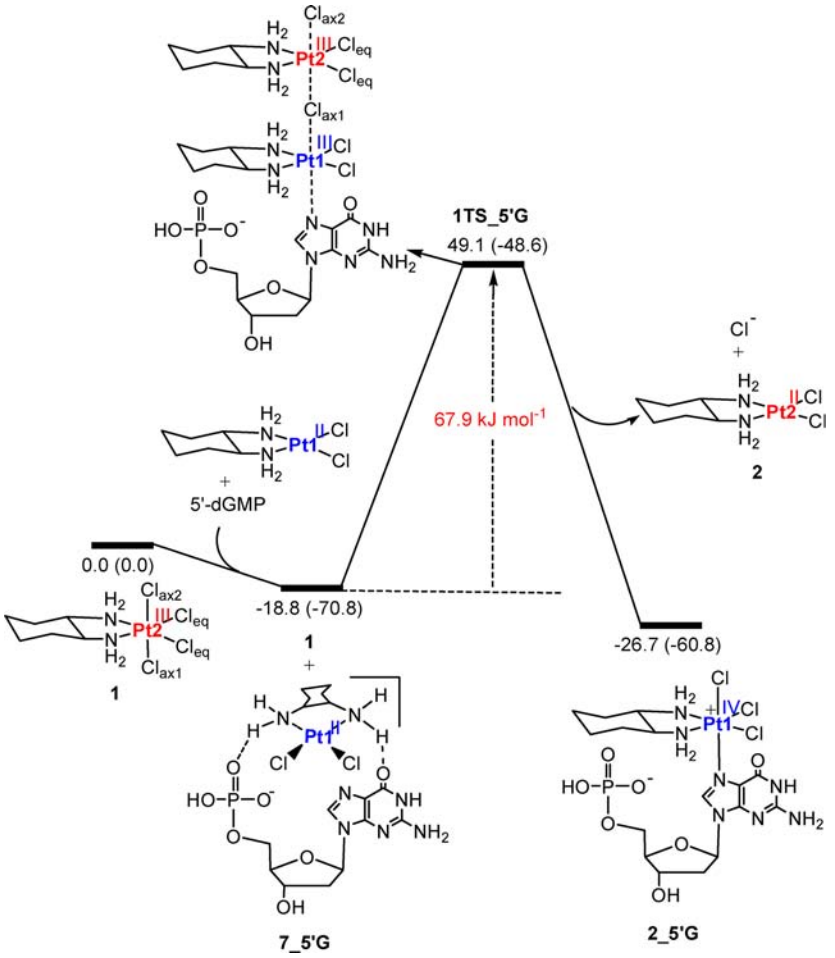

Figure 4. Energy profiles calculated for the substitution of one of the Cl_{ax} ligands of **1** by 5′-dGMP through the Pt^{II}-catalyzed pathway. The relative free and electronic energies (in parentheses) obtained from the M06/BS2//B3LYP/BS1 calculations in water are given in kJ mol^{-1}.

experimental activation energies at 298.15 K are 69.1 and 68.1 kJ mol^{-1} for the substitution reactions of 5′-dGMP and 3′-dGMP, respectively.[4e]

Oxidation of 3′-dGMP. As stated in the Introduction, after substitution of a Cl_{ax} ligand by 3′-dGMP, the G moiety can be oxidized by the nucleophilic attack of the alcohol functional group to C8 followed by the transfer of two electrons from G to Pt^{IV} and deprotonation of both the C8−H and O−H bonds. In the case of 5′-dGMP, we found that the 5′-phosphate group attacks at C8, giving the cyclic intermediate **3_5′G** (Scheme 1) with appropriate stability in order to undergo the redox reaction. By way of contrast, our calculations show that the alcohol functional group in 3′-dGMP cannot act as a nucleophile to interact with C8. Indeed, attempts to optimize **5_3′G** (Scheme 4) were unsuccessful and led to the spontaneous rearrangement to **2_3′G**. However, we could partially optimize this structure by fixing the C8−O bond at 1.431 Å[24] and found that this constrained structure is extremely unstable and lies 220.4 kJ mol^{-1} above **2_3′G** (Scheme 4). This result suggests that the alcohol functional group is not basic enough to undergo a direct attack to C8. However, one may expect that the water solvent may increase the basicity of the OH group by abstracting its proton. A three-water cluster was considered to investigate deprotonation of the hydroxyl group. Our calculations show that the C8−O bond formation following water-assisted deprotonation of the OH group leads to a relatively unstable intermediate (see **6_3′G** in Scheme 4).

Scheme 4

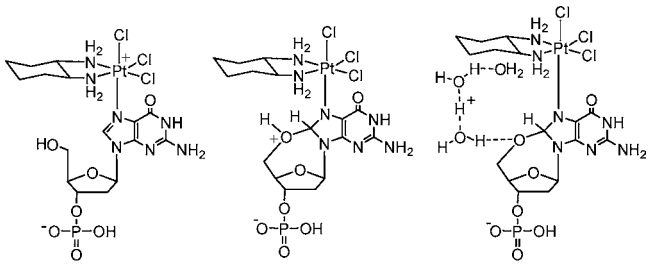

The stability of this intermediate relative to **2_3′G** + $(H_2O)_3$ is calculated to be 140.3 kJ mol^{-1}, a free energy value that is much higher than the experimental free energy reported for the oxidation of 3′-dGMP ($\Delta G^{\ddagger}$ = 97.1 kJ mol^{-1} at 298.15 K).[4e] It follows from this result that water alone is not sufficiently basic to deprotonate the hydroxyl group and, consequently, does not produce a stable intermediate for the C8−O bond formation reaction.

Our efforts in this regard finally led to an intriguing result. We found that if the water cluster $(H_2O)_3$ forms a hydrogen bond with the phosphate group, the C8−O bond-forming process is extremely facilitated (Figure 5a). In such a case, the

dx.doi.org/10.1021/ic3018425 | Inorg. Chem. 2013, 52, 707−717

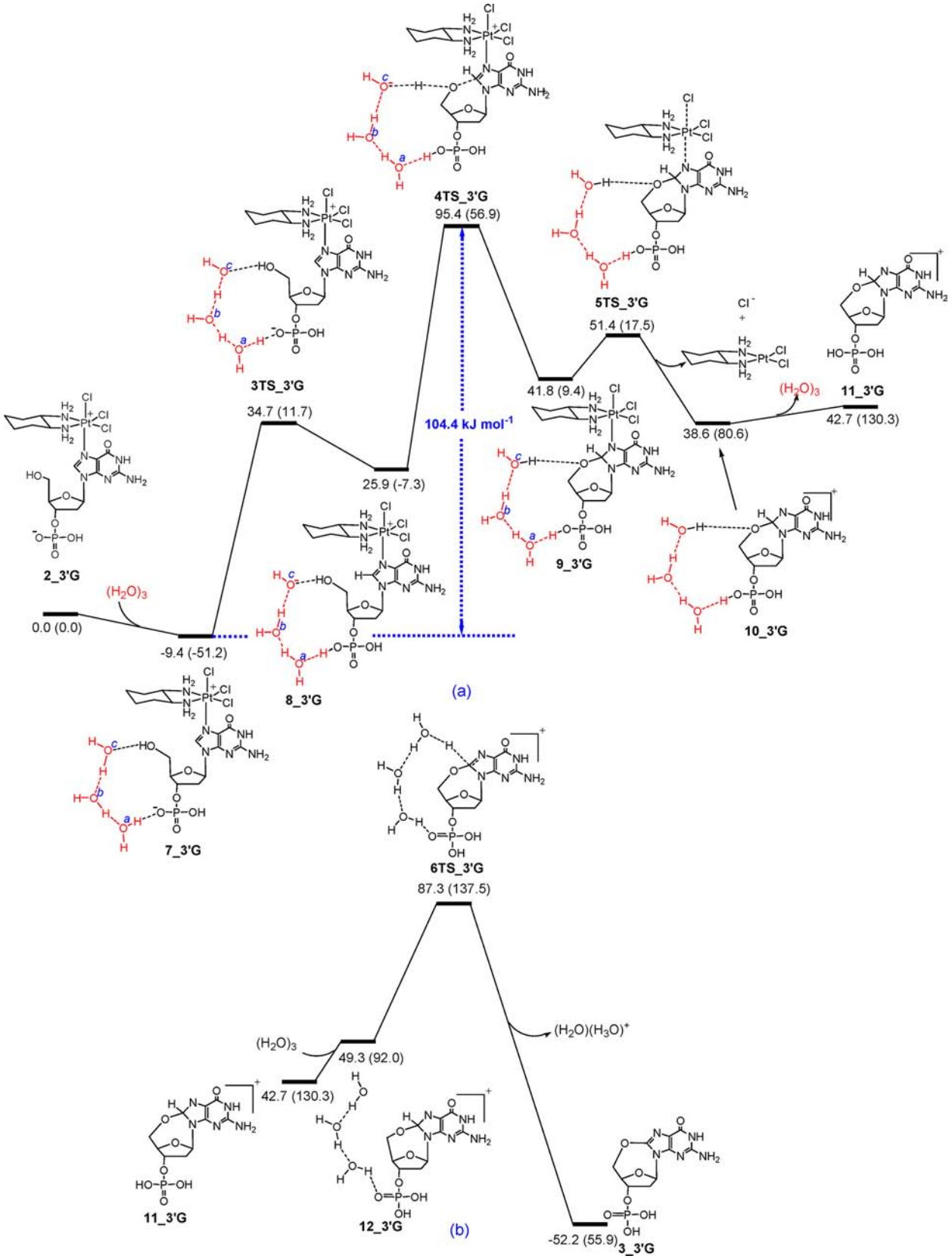

Figure 5. Energy profile calculated for the oxidation of 3′-dGMP by **1**, leading to (a) the formation of the cationic intermediate **11_3′G** and subsequently to (b) **3_3′G** through deprotonation of **11_3′G** by water. The relative free and electronic energies (in parentheses) obtained from the M06/BS2//B3LYP/BS1 calculations in water are given in kJ mol^{-1}.

reaction proceeds via a two-step mechanism. First, the phosphate group acts as a proton acceptor and through the transition structure **3TS_3′G** abstracts a proton from H_2O^a. Through this process, the deprotonation of H_2O^a by phosphate

dx.doi.org/10.1021/ic3018425 | *Inorg. Chem.* 2013, 52, 707−717

Scheme 5

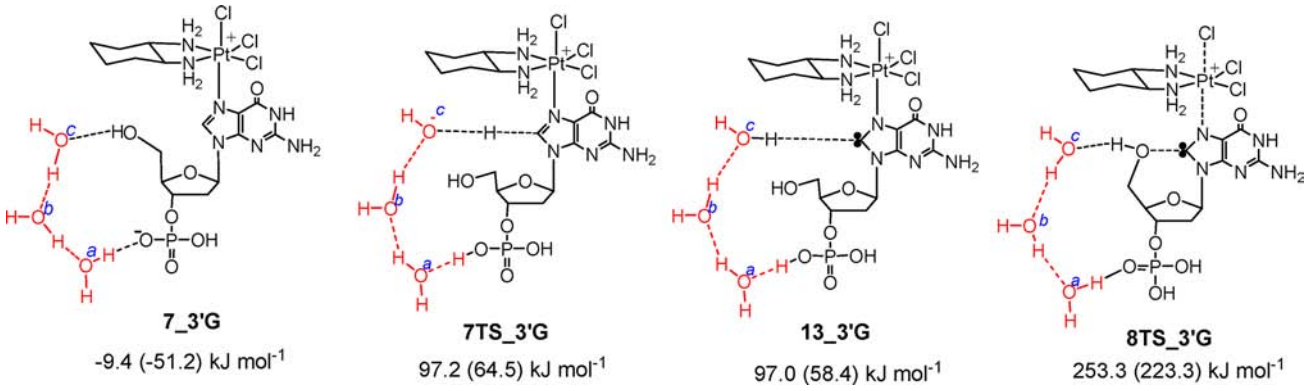

causes O^a to abstract a proton from O^b and O^b to abstract a proton from O^c, producing **8_3′G** with a hydroxide group (O^cH^-) in the vicinity of the alcohol functional group (Figure 5a). The resulting O^cH^- group in **8_3′G** is greatly stabilized by hydrogen-bonding interactions with three different groups: (a) H_2O^b, (b) NH_2 of the dach ligand, and (c) the hydroxyl group. Second, the C8−O bond-forming process (formation of **9_3′G**) can progress from **8_3′G** via the transition structure **4TS_3′G** with an activation energy as low as 69.5 kJ mol^{-1}.[25] In this transition structure, the C8−O bond is being formed concomitantly with deprotonation of the hydroxyl group by the O^cH^- anion.[26] In such a case, the reaction of **2_3′G** + $(H_2O)_3$ → **9_3′G** is not very endothermic; intermediate **9_3′G** is only 41.8 kJ mol^{-1} above **2_3′G**. This means that this reaction is 98.5 kJ mol^{-1} less endothermic than the reaction of **2_3′G** + $(H_2O)_3$ → **6_3′G**. These results show that the in situ formed hydroxide ion, which is produced by the interaction of $(H_2O)_3$ with the phosphate group, dramatically promotes the C8−O bond formation reaction. This promotion is mainly due to the high basicity of the hydroxide ion (O^cH^-).

Once **9_3′G** has formed, the G moiety of 3′-dGMP is oxidized by elongation of the Pt−Cl_{ax} bond via the transition structure **5TS_3′G**, resulting in the fragmentation of **9_3′G** into Cl^-, [Pt^{II}(dach)Cl_2], and cationic cyclic ether **10_3′G** (Figure 5a). The C8−O bond-forming process causes the HOMO of the cyclic ether moiety in **9_3′G** to lie much higher in energy than the HOMO of the 3′-dGMP moiety in **8_3′G**, and as a result, this moiety turns into a very strong reducing agent; the HOMOs of the cyclic ether and 3′-dGMP moieties exhibit energies of −3.04 and −5.69 eV, respectively. The elongation of the Pt−Cl_{ax} bond, which increases the electron-accepting ability of Pt^{IV} by stabilizing the LUMO of the [$PtCl_3$(dach)]$^+$ moiety, promotes the transfer of two electrons from G to Pt^{IV}.[27] The charge transfer from the cyclic ether moiety to the Pt d_{z^2} orbital is the main driving force for simultaneous elongation of both the Pt−Cl_{ax} and Pt−N7 bonds during the redox reaction; the d_{z^2} orbital population changes from 1.350 in **9_3′G** to 1.447 in **5TS_3′G** and then to 1.875 in **2**. These results suggest that the Pt^{IV} metal center in the transition structure **5TS_3′G** is only partially reduced. The complete occupation of the d_{z^2} orbital at the end of the redox step results in cleavage of both the Pt−Cl_{ax} and Pt−N7 bonds. Finally, the released cationic cyclic ether **11_3′G** is deprotonated by water and produces the cyclic ether **3_3′G** as the final product (Figure 5b).

The key points raised by our calculations are as follows. The production of the cyclic ether from **2_3′G** is an exergonic process and requires an overall energy barrier of 104.4 kJ mol^{-1} (Figure 5). The nucleophilic attack of the hydroxyl group to C8, which is facilitated by the in situ formed hydroxide, is the rate-determining step. This computed barrier height (104.4 kJ mol^{-1}) is in good agreement with the experimental Gibbs activation energy derived by Choi et al. (97.1 kJ mol^{-1} at 298.15 K).[4e]

In contrast to the case of 3′-dGMP, we obtained a different result for the oxidation of 5′-dGMP at the M06 level of theory;[28] the transition structure for the redox step of 5′-dGMP lies 8.4 kJ mol^{-1} above the transition structure of phosphate attack at C8. This difference can be explained in terms of the relative stabilities of **9_3′G** (Figure 5) and **3_5′G** (Scheme 1); the transition structure of the nucleophilic attack step for the case of 3′-dGMP (**4TS_3′G**) lies 53.6 kJ mol^{-1} above **9_3′G**, while the analogous transition structure for the case of 5′-dGMP only lies 7.4 kJ mol^{-1} above **3_5′G**. The higher relative stability of **9_3′G** compared to **3_5′G** is most likely due to the stronger C−O bond in **9_3′G**.

Alternative Mechanism for the Oxidation of 3′-dGMP. We also explored an alternative reaction mechanism in which the G moiety is oxidized via the initial C8−H deprotonation by the hydroxide ion O^cH^-, followed by the hydroxyl attack and redox reaction (Scheme 5). Deprotonation of the C8−H bond that occurs via the transition structure **7TS_3′G** ($\Delta G^{\ddagger}$ = 106.8 kJ mol^{-1}) is calculated to be very endergonic (ΔG = 106.6 kJ mol^{-1}). After C8−H deprotonation, the C8−O bond is formed concomitantly with G oxidation through the transition structure **8TS_3′G**. Our calculations show that **8TS_3′G** lies 157.9 kJ mol^{-1} higher in energy than **4TS_3′G**, indicating that this mechanism is unlikely to occur.[29] This transition structure lies very high in energy because, on the one hand, the deprotonation reaction is very endergonic and, on the other hand, deformation of the platinum complex in this transition structure is very significant. This is because the hydroxyl attack to C8 and G oxidation via this mechanism proceed in one step. The greater deformation in **8TS_3′G** is reflected in the longer Pt−Cl_{ax} and Pt−N7 bond distances; the Pt−Cl_{ax} and Pt−N7 bonds in **8TS_3′G** are 2.898 and 2.449 Å, respectively, while those in **4TS_3′G** are 2.411 and 2.095 Å, respectively.

Substitution of Cl by 3′-dGMP in 2. As stated in the Introduction, the Pt^{II}-catalyzed substitution reaction is in competition with the associative Cl substitution in **2**. We found that the substitution of Cl by 3′-dGMP occurs from intermediate **4_3′G** by crossing the transition structure **9TS_3′G** (Scheme 6). The overall activation barrier for this process is calculated to be 81.1 kJ mol^{-1}. The calculations at the

dx.doi.org/10.1021/ic3018425 | Inorg. Chem. 2013, 52, 707−717

Scheme 6

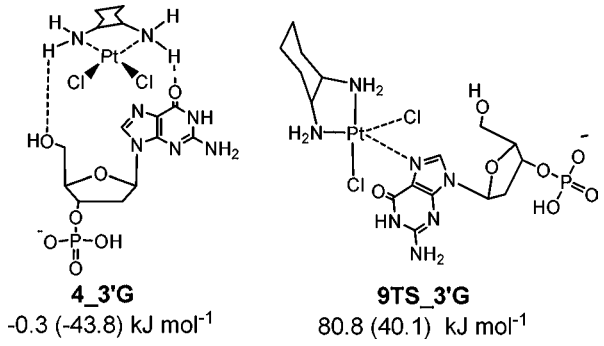

M06 level of theory suggest that the formation of [Pt(5′-dGMP)Cl(dach)] should proceed slower than the formation of [Pt(5′-dGMP)Cl_3(dach)]; the required reaction barrier for the substitution reaction catalyzed by Pt^{II} is calculated to be 67.6 kJ mol^{-1} (Figure 1). Therefore, it is expected from these results that the [$PtCl_2$(dach)] catalyst formed during the overall redox reaction preferentially participates in the Pt^{II}-catalyzed substitution reaction, and the associative substitution reaction is accelerated when the concentration of **1** becomes lower.

Summary of the Proposed Reaction Mechanism for G Oxidation of 3′-dGMP. The results of this study are summarized in Scheme 7. The substitution of Cl_{ax} by 3′-dGMP in [Pt^{IV}(dach)Cl_4], which is a necessary step for G oxidation, is catalyzed by complex **2** through formation of the encounter pair **4_3′G** (step A). The catalytic cycle of the substitution reaction is closed by the reaction of **4_3′G** with [$PtCl_4$(dach)] through the transition structure **1TS_3′G** and regeneration of the catalyst **2** (step B). Completion of step B leads to the formation of **2_3′G**. G oxidation of 3′-dGMP is started by the hydrogen-bonding interaction between a water

Scheme 7

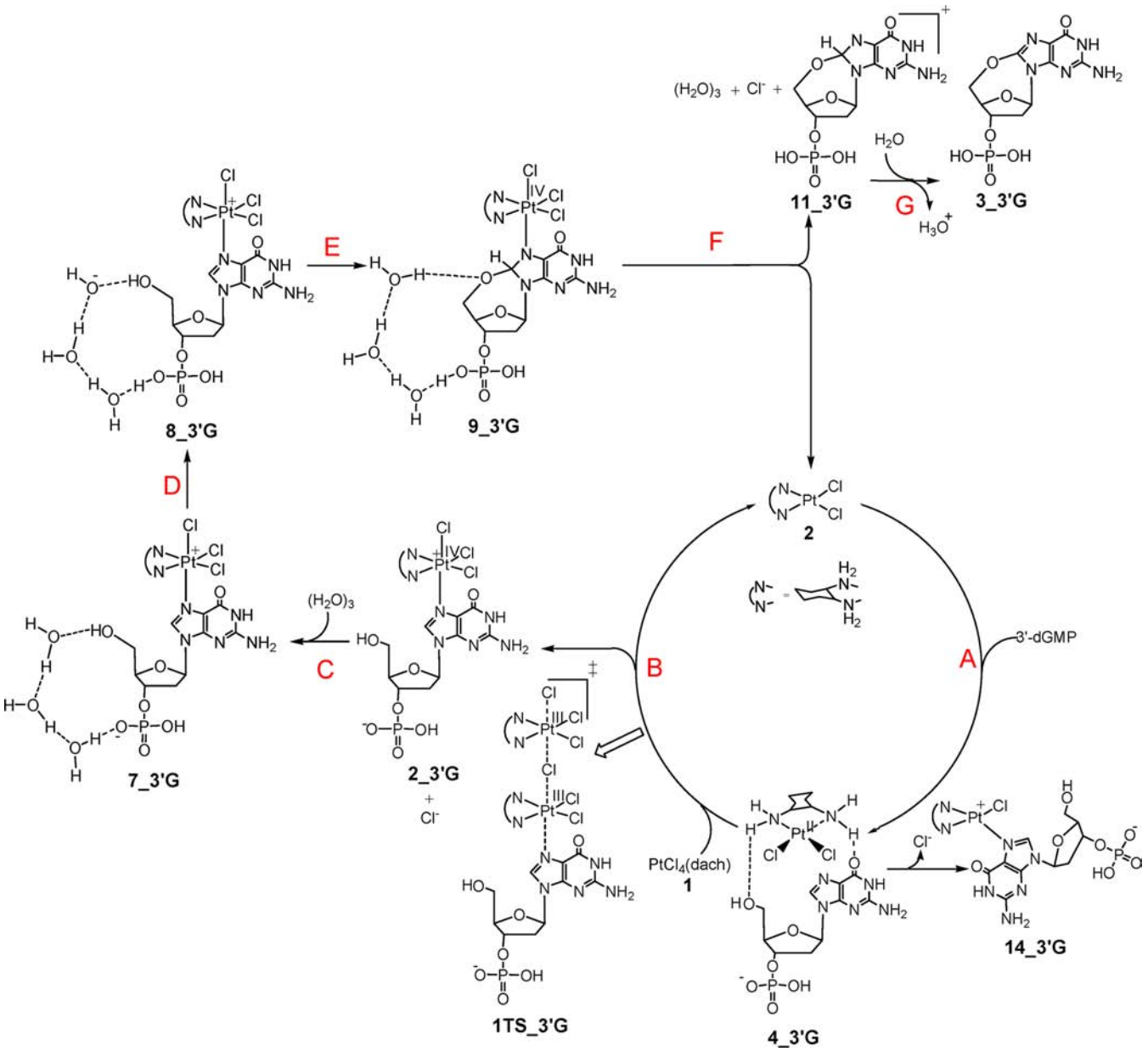

dx.doi.org/10.1021/ic3018425 | Inorg. Chem. 2013, 52, 707−717

cluster and the phosphate group of 3′-dGMP (step C). This interaction leads to the in situ formation of a hydroxide ion in the vicinity of the hydroxyl group in intermediate **8_3′G** (step D). This hydroxide ion promotes the C8−O bond formation reaction by facilitating proton abstraction from the hydroxyl group (step E). The redox step (transfer of two electrons from the G moiety of 3′-dGMP to Pt^{IV}) occurs through elongation of the $Pt^{IV}-Cl_{ax}$ bond of intermediate **9_3′G**. The complete dissociation of Cl_{ax} from **9_3′G** results in the oxidation of G by two units and the formation of the $[Pd^{II}Cl_2(dach)]$ catalyst (step F). Deprotonation of **11_3′G** by water gives the final product **3_3′G** (step G). The overall redox reaction can be called autocatalytic because the $[Pd^{II}(dach)Cl_2]$ catalyst is formed as one of the final products of the redox reaction.

An associative substitution reaction, leading to the formation of **14_3′G**, may act as a competitive process against the Pt^{II}-catalyzed substitution reaction. Our calculations predict that the associative substitution reaction is retarded in the presence of $[PtCl_4(dach)]$ because the Pt^{II}-catalyzed substitution reaction is calculated to be faster.

The main conclusion of our study is that G oxidation through the cyclization reaction is facilitated if deprotonation of the hydroxyl group is carried out by a strong hydroxide base.[30] This statement is supported by Choi et al.'s findings,[3k] which demonstrated that the production of cyclic 5′-O−C8−dGuo from $[Ru(NH_3)_5(dGuo)]$ (Scheme 8) is fast if the pH is high.

Scheme 8

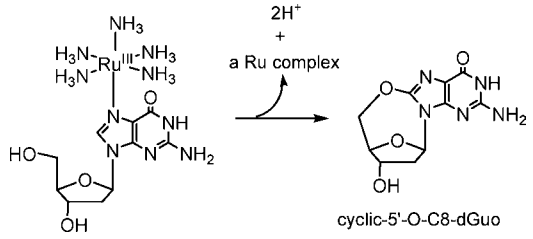

They demonstrated that the cyclization is accelerated by increased OH^- concentration.[3k] In contrast, G oxidation of 3′-dGMP by Pt^{IV} occurs easily at the relatively low pH of 8.3 because the phosphate group of 3′-dGMP enables the formation of a hydroxide ion (supported by a hydrogen-bonding network to the phosphate group) in the vicinity of the hydroxyl group.

■ ASSOCIATED CONTENT

Supporting Information

Text giving the complete ref 10, tables giving Cartesian coordinates of all optimized structures along with energies, and an additional scheme. This material is available free of charge via the Internet at http://pubs.acs.org.

■ AUTHOR INFORMATION

Corresponding Author

*E-mail: ariafard@yahoo.com (A.A.), E-Mail: Brian.Yates@utas.edu.au (B.F.Y.).

Notes

The authors declare no competing financial interest.

■ ACKNOWLEDGMENTS

This study is the result of a research project titled "Theoretical investigation into the reduction mechanism of Pt^{IV} to Pt^{II} through different pathways with the aim of producing new products". We thank the Islamic Azad University for providing funding to support this research project. We also appreciate the financial supports from the Australian Research Council and the Australian National Computational Infrastructure and the University of Tasmania for computing resources.

■ REFERENCES

(1) (a) Cadet, J.; Douki, T.; Ravanat, J.-L. *Acc. Chem. Res.* **2008**, *41*, 1075. (b) Kanvah, S.; Joseph, J.; Schuster, G. B.; Barnett, R. N.; Cleveland, C. L.; Landman, U. *Acc. Chem. Res.* **2010**, *43*, 280.

(2) (a) Kawanishi, S.; Hiraku, Y.; Oikawa, S. *Mutat. Res., Rev. Mutat. Res.* **2001**, *488*, 65. (b) Wallace, S. S. *Free Radical Biol. Med.* **2002**, *33*, 1. (c) Franco, R.; Schoneveld, O.; Georgakilas, A. G.; Panayiotidis, M. I. *Cancer Lett.* **2008**, *266*, 6.

(3) (a) Roat, R. M.; Reedijk, J. *J. Inorg. Biochem.* **1993**, *52*, 263. (b) Muller, J. G.; Zheng, P.; Rokita, S. E.; Burrows, C. J. *J. Am. Chem. Soc.* **1996**, *118*, 2320. (c) Rodriguez-Bailey, V. M.; LaChance-Galang, K. J.; Doan, P. E.; Clarke, M. J. *Inorg. Chem.* **1997**, *36*, 1873. (d) Burrows, C. J.; Muller, J. G. *Chem. Rev.* **1998**, *98*, 1109. (e) Farrer, B. T.; Thorp, H. H. *Inorg. Chem.* **2000**, *39*, 44. (f) Farrer, B. T.; Thorp, H. H. *Inorg. Chem.* **2000**, *39*, 44. (g) Williams, T. T.; Dohno, C.; Stemp, E. D. A.; Barton, J. K. *J. Am. Chem. Soc.* **2004**, *126*, 8148. (h) Li, L.; Karlin, K. D.; Rokita, S. E. *J. Am. Chem. Soc.* **2005**, *127*, 520. (i) Pratviel, G.; Meunier, B. *Chem.—Eur. J.* **2006**, *12*, 6018. (j) Olmon, E. D.; Sontz, P. A.; Blanco-Rodríguez, A. M.; Towrie, M.; Clark, I. P.; Vlček, A., Jr.; Barton, J. K. *J. Am. Chem. Soc.* **2011**, *133*, 13718. (k) Choi, S.; Ryu, D. W.; DellaRocca, J. G.; Wolf, M. W.; Bogart, J. A. *Inorg. Chem.* **2011**, *50*, 6567. (l) Olmon, E. D.; Hill, M. G.; Barton, J. K. *Inorg. Chem.* **2011**, *50*, 12034.

(4) (a) Choi, S.; Filotto, C.; Bisanzo, M.; Delaney, S.; Lagasee, D.; Whitworth, J. L.; Jusko, A.; Li, C.; Wood, N. A.; Willingham, J.; Schwenker, A.; Spaulding, K. *Inorg. Chem.* **1998**, *37*, 2500. (b) Choi, S.; Mahalingaiah, S.; Delaney, S.; Neale, N. R.; Masood, S. *Inorg. Chem.* **1999**, *38*, 1800. (c) Choi, S.; Cooley, R. B.; Hakemian, A. S.; Larrabee, Y. C.; Bunt, R. C.; Maupaus, S. D.; Muller, J. G.; Burrows, C. J. *J. Am. Chem. Soc.* **2004**, *126*, 591. (d) Choi, S.; Cooley, R. B.; Voutchkova, A.; Leung, C. H.; Vastag, L.; Knowles, D. E. *J. Am. Chem. Soc.* **2005**, *127*, 1773. (e) Choi, S.; Vastag, L.; Leung, C. H.; Beard, A. M.; Knowles, D. E.; Larrabee, J. A. *Inorg. Chem.* **2006**, *45*, 10108. (f) Choi, S.; Vastag, L.; Larrabee, Y. C.; Personick, M. L.; Schaberg, K. B.; Fowler, B. J.; Sandwick, R. K.; Rawji, G. *Inorg. Chem.* **2008**, *47*, 1352. (g) Choi, S.; Personick, M. L.; Bogart, J. A.; Ryu, D. W.; Redman, R. M.; Laryea-Walker, E. *Dalton Trans.* **2011**, *40*, 2888.

(5) Hall, M. D.; Hambley, T. W. *Coord. Chem. Rev.* **2002**, *232*.

(6) Chaney, S. G.; Wyrick, S.; Till, G. K. *Cancer Res.* **1990**, *50*, 4539.

(7) Ariafard, A.; Tabatabaie, E. S.; Aghmasheh, S.; Najaflo, S.; Yates, B. F. *Inorg. Chem.* **2012**, *51*, 8002.

(8) (a) Basolo, F.; Wilks, P. H.; Pearson, R. G.; Wilkins, R. G. *J. Inorg. Nucl. Chem.* **1958**, *6*, 161. (b) Basolo, F.; Morris, M. L.; Pearson, R. G. *Discuss Faraday Soc.* **1960**, *29*, 80. (c) Ellison, H. R.; Asolo, F.; Pearson, R. *J. Am. Chem. Soc.* **1961**, *83*, 3943. (d) Basolo, F.; Pearson, R. G. *Adv. Inorg. Chem. Radiochem.* **1961**, *3*, 1. (e) Cox, L. T.; Collins, S. B.; Martin, D. S. *J. Inorg. Nucl. Chem.* **1961**, *17*, 383. (f) Mason, W. R. *Coord. Chem. Rev.* **1972**, *7*, 241. (g) Summa, G. M.; Scott, B. A. *Inorg. Chem.* **1980**, *19*, 1079.

(9) (a) Davies, M. S.; Hall, M. D.; Berners-Price, S. J.; Hambley, T. W. *Inorg. Chem.* **2008**, *47*, 7673. (b) Nemirovski, A.; Vinograd, I.; Takrouri, K.; Mijovilovich, A.; Rompel, A.; Gibson, D. *Chem. Commun.* **2010**, *46*, 1842. (c) McCall, A. S.; Kraft, S. *Organometallics* **2012**, *31*, 3527.

(10) Frisch, M. J.; et al. *Gaussian 09*, revision A.02; Gaussian, Inc.: Wallingford, CT, 2009.

(11) Barone, V.; Cossi, M. *J. Phys. Chem. A* **1998**, *102*, 1995.

(12) (a) Lee, C. T.; Yang, W. T.; Parr, R. G. *Phys. Rev. B* **1988**, *37*, 785. (b) Miehlich, B.; Savin, A.; Stoll, H.; Preuss, H. *Chem. Phys. Lett.* **1989**, *157*, 200. (c) Becke, A. D. *J. Chem. Phys.* **1993**, *98*, 5648.

(13) (a) Hay, P. J.; Wadt, W. R. *J. Chem. Phys.* **1985**, *82*, 270. (b) Wadt, W. R.; Hay, P. J. *J. Chem. Phys.* **1985**, *82*, 284.
(14) Hariharan, P. C.; Pople, J. A. *Theor. Chim. Acta* **1973**, *28*, 213.
(15) Ehlers, A. W.; Böhme, M.; Dapprich, S.; Gobbi, A.; Höllwarth, A.; Jonas, V.; Köhler, K. F.; Stegmann, R.; Veldkamp, A.; Frenking, G. *Chem. Phys. Lett.* **1993**, *208*, 111.
(16) (a) Fukui, K. *J. Phys. Chem.* **1970**, *74*, 4161. (b) Fukui, K. *Acc. Chem. Res.* **1981**, *14*, 363.
(17) (a) Zhao, Y.; Schultz, N. E.; Truhlar, D. G. *J. Chem. Theory Comput.* **2006**, *2*, 364. (b) Zhao, Y.; Truhlar, D. G. *J. Chem. Phys.* **2006**, *125*, 194101. (c) Zhao, Y.; Truhlar, D. G. *J. Phys. Chem. A* **2006**, *110*, 13126.
(18) Zhao, Y.; Truhlar, D. G. *Theor. Chem. Acc.* **2008**, *120*, 215.
(19) Weigend, F.; Furche, F.; Ahlrichs, R. *J. Chem. Phys.* **2003**, *119*, 12753.
(20) It is a method through which one can estimate the entropy difference between the gas and liquid phases. Okuno, Y. *Chem.—Eur. J.* **1997**, *3*, 212.
(21) Glendening, E. D.; Read, A. E.; Carpenter, J. E.; Weinhold, F. *NBO*, version 3.1; Gaussian, Inc.: Pittsburgh, PA, 2003.
(22) Although an encounter pair in which the phosphate group of 3′-dGMP is involved in hydrogen bonding with the N−H protons of the dach ligand (**4′_3′G**) is more stable than **4_3′G**, the stabilities of these two encounter pairs in the presence of water are predicted to be comparable (Scheme S1 in the SI).
(23) For detailed information, see: Albright, T. A.; Burdett, J. K.; Whangbo, M.-H. *Orbital Interactions in Chemistry*; Wiley: New York, 1985; p 330.
(24) A distance taken from the C8−O bond in **9_3′G**.
(25) This activation energy (69.5 kJ mol^{-1}) becomes even lower when the G moiety of 3′-dGMP is replaced by hypoxanthine (see Figure S1 in the SI and its associated discussion for more details). This replacement increases the electron deficiency of C8 and facilitates the nucleophilic attack of the hydroxyl group at C8.
(26) The C8−O bond formation through deprotonation of the hydroxyl group by the phosphate without the aid of water is very energy-consuming. The transition structure for this pathway (**4′TS_3′G**) lies 60.4 kJ mol^{-1} above **4TS_3′G**, indicating the essential role of the water in favoring the C8−O bond formation step. This pathway is disfavored because the O atom of the phosphate in **2_3′G** is quite far away from C8 (4.726 Å).

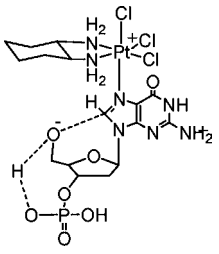

4'TS_3'G
155.8 (155.8) kJ mol^{-1}

(27) For a detailed discussion of the redox mechanism, see ref 7.
(28) Figure S2 in the Supporting Information of ref 7.
(29) A related mechanism in which the cyclization reaction is initiated via C8−H deprotonation by a solvent prior to the hydroxyl attack to C8 was also investigated. Our calculations show that this mechanism for the oxidation of 3′-dGMP is energetically unfavorable (see Scheme S2 in the SI and its associated discussion).
(30) The argument for acceleration of the cyclization step by a strong hydroxide base is supported by calculations of the cyclization reaction assisted by $(H_2O)_3$ and $(H_2O)_2(OH^-)$ for $[Pt^{IV}(dach)(dGuo)Cl_3]^+$ (dGuo = deoxyguanosine). Our calculations predict that the corresponding reaction is much faster in basic media (see Scheme S3 in the SI and its associated discussion).